Theory of optical spectra of exciton condensates

H. Chu and Y. C. Chang

Department of Physics and Materials Research Laboratory, University of Illinois at Urbana-Champaign,
1110 West Green Street, Urbana, Illinois 61801-3080

(Received 27 December 1995)

We present theoretical calculations of optical absorption-gain spectra for condensed excitons in both three dimensional (3D), 2D, and quasi-2D systems (appropriate for semiconductor quantum wells) as functions of the electron-hole pair density and temperature. The ladder diagram contribution to the vertex function (exciton effect) is included in our calculation. We found that fluctuations cannot destroy the condensation of excitons in 2D at finite temperatures as opposed to a theory of free bosons and the case of Cooper pairs in superconductivity. Such a difference is attributed to the fact that electrons and holes carry opposite charges as opposed to the same charges carried by the Cooper pairs in the case of superconductivity. Our studies show that the effects of exciton Bose condensation on the absorption-gain spectra remain present for temperatures up to 130 K for a 2D system with exciton binding energy of 30–40 meV (appropriate for ZnSe systems). [S0163-1829(96)08531-1]

I. INTRODUCTION

Recently there has been renewed interest in Bose-Einstein condensations generated by the observation of such phenomena in exciton systems[1] and atomic systems[2] with very weak interboson interactions. The condensation of composite bosons is thoroughly studied for Cooper pairs in the phenomena of superconductivity[3] and of excitons in optically excited semiconductors.[4–9] Qualitative behavior of exciton condensed systems has been analyzed in the high- and low-density limits. However, a realistic quantitative study of exciton condensations at finite temperature is still lacking. This is of particular importance in light of recent advances of semiconductor lasers in the blue-green regime[8] in which the exciton condensation will play a role in the lasing mechanism at least at lower temperatures (<100 K). The gap equation for ideal two-dimensional 2D and quantum well (quasi-2D) systems at $T=0$ has been solved numerically in Ref. 7. Recently, Flatté *et al.* studied the optical properties at $T=0$ without including the exciton effect.[9] In this paper, we not only consider the finite-temperature effects but also include the exciton effect (ladder diagram contribution to the vertex function) in calculating the optical spectra. It is found that the exciton effect is essential in determining the absorption or gain spectra at low temperatures where the exciton condensate exists.

Our calculation is based on the BCS mean-field theory in which the phase symmetry is broken; i.e., the condensate state is a superposition of states with different particle numbers. In optically excited semiconductor systems, the number of electron-hole pairs does not have to be conserved, while the total number of electrons is conserved. In this case the symmetry breaking is induced by the optical field. It has been shown that the effect of the external optical pump field is to introduce equivalent chemical potential under the so-called rotating-wave approximation, though the validity of such an approximation may be questionable.

We shall first solve the gap equation for 2D systems with different densities with a wide range of temperatures. We then calculate optical absorption (gain) spectra including the exciton effect for 3D, 2D, and quasi-2D systems (appropriate for semiconductor quantum wells). Finally we will show that fluctuations cannot destroy the condensation of excitons in 2D at finite temperature as opposed to a theory of free bosons and the case of Cooper pairs in superconductivity. Such a difference is attributed to the difference in the signs of carrier charges, electrons and holes are oppositely charged in contrast to the case of superconductivity where we have up-spin electrons and down-spin electrons. This leads to the difference in the interparticle interactions.

II. BCS THEORY FOR EXCITONS

In the BCS theory,[5] the inverse of the Green's function for electrons and holes in the exciton system is written in the 2×2 matrix form

$$G^{-1}(k_0,\mathbf{k})=\begin{pmatrix} k_0-\epsilon_1(\mathbf{k}) & -\Delta_{\mathbf{k}} \\ -\Delta_{\mathbf{k}} & k_0+\epsilon_2(\mathbf{k}) \end{pmatrix}, \qquad (1)$$

where $k_0,\mathbf{k}$ denote the frequency and wave vector, $\epsilon_1(\mathbf{k})\equiv\varepsilon_c(\mathbf{k})-\mu_1$ and $\epsilon_2(\mathbf{k})\equiv\varepsilon_h(\mathbf{k})-\mu_2$ are the electron and hole energies (including the self-energy correction) measured with respect to their corresponding chemical potentials, μ_1 and μ_2, respectively. $\Delta_{\mathbf{k}}$ is the off-diagonal part of the self-energy matrix $\Sigma(\mathbf{k})$, which is frequency independent in the Hartree-Fock mean-field approximation. $G^{-1}(k_0,\mathbf{k})$ becomes diagonalized under the Bogoliubov transformation.

$$G^{-1}(k_0,\mathbf{k})=U_{\mathbf{k}}^{\dagger}(k_0-\delta\epsilon_{\mathbf{k}}-E_{\mathbf{k}}\tau_3)U_{\mathbf{k}}, \qquad (2)$$

where $\epsilon_{\mathbf{k}}=[\epsilon_1(\mathbf{k})+\epsilon_2(\mathbf{k})]/2$, $\delta\epsilon_{\mathbf{k}}=[\epsilon_1(\mathbf{k})-\epsilon_2(\mathbf{k})]/2$, $E_{\mathbf{k}}^2=\epsilon_{\mathbf{k}}^2+\Delta_{\mathbf{k}}^2$ is the renormalized energy, and $U_{\mathbf{k}}$ is the transformation matrix defined as

$$U_{\mathbf{k}}=u_{\mathbf{k}}\tau_0-v_{\mathbf{k}}\tau_2, \qquad U_{\mathbf{k}}^{\dagger}=u_{\mathbf{k}}\tau_0+v_{\mathbf{k}}\tau_2,$$

with $u_{\mathbf{k}}^2 - v_{\mathbf{k}}^2 = \epsilon_{\mathbf{k}}/E_{\mathbf{k}}$, $2u_{\mathbf{k}}v_{\mathbf{k}} = \Delta/E_{\mathbf{k}}$. $\epsilon_{\mathbf{k}}$, $\delta\epsilon_{\mathbf{k}}$, $\Delta_{\mathbf{k}}$, μ_1, and μ_2 are to be determined from the gap equation self-consistently. Here we introduce the notations $\tau_0 = 1$, $\tau_1 = \tau_x$, $\tau_3 = \tau_z$, and $\tau_2 = -i\tau_y$, where τ_x, τ_y, and τ_z are the usual Pauli matrices. If $\Delta_{\mathbf{k}} \neq 0$ the symmetry is broken.

To make our theory applicable for both superconductivity and exciton condensation, we adopt the following general form (in terms of the Nambu notations) for the interaction Hamiltonian,

$$H_{\text{int}} = \frac{1}{2}\sum_i \int d\mathbf{x}\, d\mathbf{y}\, V(\mathbf{x}-\mathbf{y}) : \bar{\psi}(\mathbf{x})\tau_{\mathbf{i}}\psi(\mathbf{x})\bar{\psi}(\mathbf{y})\tau_{\mathbf{i}}\psi(\mathbf{y}):.$$

Here ψ is a two-component field operator. In the case of superconductivity, we only keep the τ_3 term, while in the case of the exciton system, we only keep the τ_0 term (in the original conduction-band and valence-band picture) so that

$$H_{\text{int}} = \frac{1}{2}\int d\mathbf{x}\, d\mathbf{y}\, V(\mathbf{x}-\mathbf{y}) : \bar{\psi}(\mathbf{x})\psi(\mathbf{x})\bar{\psi}(\mathbf{y})\psi(\mathbf{y}):.$$

Ignore the frequency dependence in the screening effect, the dominant term in the self-energy (for the exciton system) is given by

$$\Sigma(\mathbf{k}) = \sum_{k_0,\mathbf{q}} V_S(\mathbf{k}-\mathbf{q})G(k_0,\mathbf{q}). \tag{3}$$

Here $V_S(\mathbf{k}-\mathbf{q})$ is the Fourier transform of the statically screened electron-electron interaction, which is considered a scalar in the above matrix equation.

At finite temperatures, the integration over k_0 is replaced by a summation over the Matsubara frequencies $k_0 \rightarrow i(2n+1)\pi/\beta$ ($\beta \equiv 1/k_BT$). Carrying out the summation yields

$$\sum_{k_0} G(k_0,\mathbf{k}) = -U_{\mathbf{k}}^{\dagger}\begin{pmatrix} n_1(\mathbf{k}) & 0 \\ 0 & 1-n_2(\mathbf{k}) \end{pmatrix}U_{\mathbf{k}},$$

where $n_1(\mathbf{k}) = 1/(e^{\beta(E_{\mathbf{k}}+\delta\epsilon_{\mathbf{k}})}+1)$ and $n_2(\mathbf{k}) = 1/(e^{\beta(E_{\mathbf{k}}-\delta\epsilon_{\mathbf{k}})}+1)$. Substituting this result into Eq. (3) yields for the diagonal part

$$\epsilon_1(\mathbf{k}) = \epsilon_1^0(\mathbf{k}) - \mu_1 - \frac{1}{2}\sum_{\mathbf{q}} V_S(\mathbf{k}-\mathbf{q})\left\{ n_1(\mathbf{q}) - n_2(\mathbf{q}) + 1 \right.$$
$$\left. - [1-n_1(\mathbf{q})-n_2(\mathbf{q})]\frac{\epsilon_{\mathbf{q}}}{E_{\mathbf{q}}} \right\}, \tag{4}$$

$$\epsilon_2(\mathbf{k}) = \epsilon_2^0(\mathbf{k}) - \mu_2 - \frac{1}{2}\sum_{\mathbf{q}} V_S(\mathbf{k}-\mathbf{q})\left\{ n_2(\mathbf{q}) - n_1(\mathbf{q}) + 1 \right.$$
$$\left. - [1-n_1(\mathbf{q})-n_2(\mathbf{q})]\frac{\epsilon_{\mathbf{q}}}{E_{\mathbf{q}}} \right\}, \tag{5}$$

where $\epsilon_1^0(\mathbf{k})$ and $\epsilon_2^0(\mathbf{k})$ are the electron and hole band energies in the absence of the optical field. The last term in each of the two equations is just the Hartree-Fock exchange energy. It is more convenient to express these two equations in

terms of their average and difference. Together with the gap equation, which is obtained from equating the off-diagonal parts in Eq. (3), we obtain the complete set of self-consistent equations:

$$\epsilon_k = \epsilon_k^0 - \frac{\mu}{2} - \frac{1}{2}\sum_{\mathbf{q}} V_S(\mathbf{k}-\mathbf{q})\left\{ 1 - [1-n_1(\mathbf{q})-n_2(\mathbf{q})]\frac{\epsilon_{\mathbf{q}}}{E_{\mathbf{q}}} \right\}, \tag{6}$$

$$\delta\epsilon_k = \delta\epsilon_k^0 - \delta\mu + \frac{1}{2}\sum_{\mathbf{q}} V_S(\mathbf{k}-\mathbf{q})[n_2(\mathbf{q})-n_1(\mathbf{q})], \tag{7}$$

$$\Delta_{\mathbf{k}} = \frac{1}{2}\sum_{\mathbf{q}} V_S(\mathbf{k}-\mathbf{q})[1-n_1(\mathbf{q})-n_2(\mathbf{q})]\frac{\Delta_{\mathbf{q}}}{E_{\mathbf{q}}}, \tag{8}$$

$$E_{\mathbf{k}}^2 = \epsilon_{\mathbf{k}}^2 + \Delta_{\mathbf{k}}^2, \tag{9}$$

$$\sum_{\mathbf{k}} n_1(\mathbf{k}) = \sum_{\mathbf{k}} n_2(\mathbf{k}). \tag{10}$$

In solving these equations, the easiest approach is to first fix the exciton chemical potential μ. However, $\delta\mu$ must be varied to ensure that Eq. (10) holds. This is the most difficult part of our problem. If the masses of the conduction band and valence band are equal, then Eqs. (8) and (10) will not be needed and the numerical computation will be much easier. Since the qualitative behavior of exciton condensation is insensitive to the difference in electron and hole effective masses, we shall only consider the equal-mass case at finite temperatures in the present paper. At $T=0$, it can be easily shown that it is still self-consistent to assume that $\delta\mu=0$ so that $n_1(\mathbf{k}) = n_2(\mathbf{k}) = 0$, so the results are independent of the electron-to-hole mass ratio after the energy is scaled according to the exciton Rydberg (Ry).

At zero temperature, there is no unpaired electrons and holes, we therefore ignore the screening effect. At finite temperatures, there is strong screening effect due to unpaired electrons and holes, we shall therefore include the screening in the above self-consistent equations. If we ignore the ladder diagram, the long-wavelength limit of the polarization (density-density correlation) function can be expressed as (derivations will be given in the next section when the vertex function is discussed)

$$\Pi_0 = -2\sum_{\mathbf{k}} dn(\mathbf{k})/dE_{\mathbf{k}} = 2\beta\sum_{\mathbf{k}} e^{-\beta E_{\mathbf{k}}}/(1+e^{-\beta E_{\mathbf{k}}})^2.$$

The screened interaction is then written as

$$V_S(q) = V_{\mathbf{q}}/(1+\Pi_0 V_{\mathbf{q}}),$$

where $V_{\mathbf{q}}$ is the bare interaction. In an ideal 2D system, the bare interaction is written as a/q (a is a constant), and the screened interaction will be written as $a/(q+a\Pi_0)$. There is no screening at $T=0$. This can be explained by the fact there are no free electrons and holes in the present approximation at $T=0$ since they all form pairs and are condensed. There are no free charge carriers in large distance scale since exci-
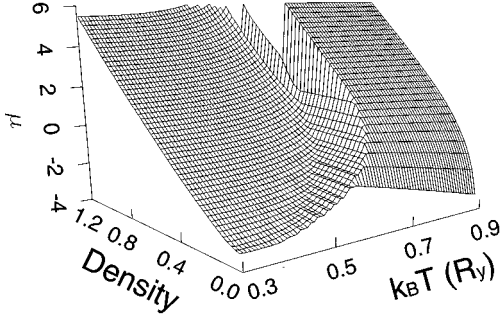
FIG. 1. 3D plot for chemical potential and electron-hole pair density vs temperature of the exciton condensate in an ideal 2D system with static screening.
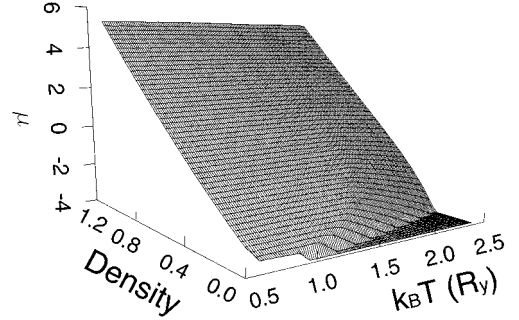

FIG. 2. 3D plot for chemical potential and electron-hole pair density vs temperature of the exciton condensate in an ideal 2D system without screening.

tons are neutral and therefore screening is very ineffective. When $T>0$, there will be thermally excited free electrons and holes and the screening becomes finite at $\mathbf{q}=0$. However, at short distances (which correspond to $q>0$), the screening is indeed possible even when $T=0$. Hence we are still underestimating screening effects at finite $\mathbf{q}$ when there are condensed excitons. We shall not be too concerned by this since a truly satisfactory theory should also include both dynamical screening and vertex corrections (which must be guided by Ward-Takahashi identities). Such an ambitious task will be left as a subject of future research.

The screening and pairing depend on each other and they are determined by solving the set of self-consistent equations. In the numerical solution of the gap equations, we fix the exciton chemical potential and the temperature and solve the problem iteratively. A 3D plot of the chemical potential versus temperature and density is in Fig. 1 for an ideal 2D exciton system where the masses of the conduction band and valence band are assumed equal. The screening effect due to unpaired electrons and holes is included. In this plot, the temperature is measured in units of Ry/k_B. Throughout this paper, the energy unit is exciton Rydberg, $\mathrm{Ry}=13.6$ eV $\times (\mu^*/m_0)/\epsilon_0^2$, where μ^* is the effective electron-hole reduced mass, m_0 is the bare electron mass, and ϵ_0 is the static dielectric constant of the semiconductor. The total pair density is defined as

$$N_0 = \sum_{\mathbf{k}} \frac{1}{2} \left[1 - [1 - 2n(\mathbf{q})] \frac{\epsilon_q}{E_q} \right]$$

and it is measured in units of a_B^{-2} where $a_B = 0.529$ Å $\times \epsilon_0/(\mu^*/m_0)$. For GaAs (ZnSe), we have Ry ≈ 4 meV (17 meV) and $a_B \approx 150$ Å (45 Å). The phase transition temperature can be identified for each density on the plot, which increases when the density of the electron-hole pair is increased. At larger densities the transition becomes very sharp and becomes first-order-like. In the course of our calculation, we find that the solution is rather sensitive to the initial input for the various parameters. A bad initial input can lead to a solution with no condensation of excitons. This is very much different from the zero-temperature calculation where any initial setup of the parameters can lead to the solution with condensation of excitons whenever such a solution does exist. Our calculation shows that the highest transition temperature is around 30 K (130 K) for GaAs (ZnSe) 2D system. It

is also important to point out that without including the screening effect, the transition temperature is much higher and the solution is much more stable. For comparison, we present the results of our calculations with no screening effect in Fig. 2. It can be seen that the transition temperature is much higher (about a factor 2), which is expected since the interaction is stronger without screening. The other noted difference is that the phase transition is much smoother compared to the case with screening. This can be explained as follows. Consider the case with screening, as we lower the temperature from above T_c to below T_c, the pair condensation tends to suppress screening, which in turn reinforces condensation, thus giving rise to a sharper phase transition.

III. OPTICAL SPECTRA

To calculate optical spectra, we use the ladder diagrams, following the recipes proposed by Baym and Kadanoff,[10] to ensure that the correlation function satisfies the conservation law and qualitatively good optical spectra. For instance, there must exist an exciton mode whose energy approaches that of the condensed exciton energy, which is equal to the chemical potential at wave vector $\mathbf{k}=0$ in accord with the so-called Goldstone theorem.

For optical transition processes the interaction Hamiltonian is written as

$$\sum_{\mathbf{k}} P_{\mathbf{q}}(\mathbf{k})(a_{\mathbf{k}+\mathbf{q}}^{\dagger} b_{\mathbf{k}} + b_{\mathbf{k}}^{\dagger} a_{\mathbf{k}+\mathbf{q}}) \equiv \sum_{\mathbf{k}} P_{\mathbf{q}}(\mathbf{k})$$
$$\times (\bar{\psi}_{\mathbf{k}+\mathbf{q}} \tau^{+} \psi_{\mathbf{k}} + \bar{\psi}_{\mathbf{k}} \tau^{-} \psi_{\mathbf{k}+\mathbf{q}}),$$

where $P_{\mathbf{q}}(\mathbf{k})$ is the momentum matrix element between states $\mathbf{k}$ and $\mathbf{k}+\mathbf{q}$ and $\psi_{\mathbf{k}}$ is a two-component field operator, $(a_{\mathbf{k}}, b_{\mathbf{k}})$.

The absorption coefficient is proportional to the imaginary part of the current-current correlation function $\pi(q)$, which can be written in terms of the three-point vertex function [here denoted by $\Gamma_q(k)$] as[11]

$$\pi(q) = \mathrm{Tr} \left\{ \sum_k [\Gamma_q^0(k)]^{\dagger} G(k) \Gamma_q(k) G(k-q) \right\}. \quad (11)$$

Here, for simplicity, we have introduced the 4-vector notations $q=(q_0, \mathbf{q})$ and $k=(k_0, \mathbf{k})$. The subscript q for Γ cor-

responds to the 4-vector of the incident photon in the optical transition process. Γ^0 is the bare vertex function, which is simply $\Gamma_q^0(k)=P_{\mathbf{q}}(\mathbf{k})\tau^{\pm}$, where $+(-)$ corresponds to the absorption (emission) process. Since both the Green's function and the vertex function are 2×2 matrices it is important to keep them in the correct order. In the ladder diagram approximation, $\Gamma_q(k)$ satisfies the following equation:

$$\Gamma_q(k)=\Gamma_q^0(k)+\sum_i\sum_{\mathbf{k}'}\left[\tau_i\sum_{k_0'}G(k')\Gamma_q(k')\right.$$
$$\left.\times G(k'-q)\tau_i\right]V_i(\mathbf{k}-\mathbf{k}'). \qquad (12)$$

Here again, we only keep the τ_0 term for excitons and the τ_3 term for Cooper pairs.

To explicitly calculate the vertex function $\Gamma_q(k)$, we need the following relations for the Bogoliubov transformation matrices

$$U_1^{\dagger}(\tau_0,\tau_2)U_2=(\tau_0,\tau_2)\begin{pmatrix}C^- & -S^- \\ S^- & C^-\end{pmatrix},$$

$$U_1^{\dagger}(\tau_1,\tau_3)U_2=(\tau_1,\tau_3)\begin{pmatrix}C^+ & S^+ \\ -S^+ & C^+\end{pmatrix},$$

where $C^{\pm}\equiv u_1u_2\mp v_1v_2$ and $S^{\pm}\equiv v_1u_2\pm v_2u_1$. Here the subscripts 1 and 2 are abbreviations for the wave vectors $\mathbf{k}$ and $\mathbf{k}+\mathbf{q}$, respectively. Let $\mathcal{E}_1(\mathbf{k})\equiv E_{\mathbf{k}}+\delta\epsilon_{\mathbf{k}}$ and $\mathcal{E}_2(\mathbf{k})\equiv E_{\mathbf{k}}-\delta\epsilon_{\mathbf{k}}$, we get after summation over the Matsubara frequencies

$$\sum_{k_0}G(k)(\tau_0,\tau_3)G(k-q)=U_1^{\dagger}(\tau_0,\tau_3)\begin{pmatrix}A_1 & A_2 \\ A_2 & A_1\end{pmatrix}U_2,$$

$$\sum_{k_0}G(k)(\tau_2,\tau_1)G(k-q)=U_1^{\dagger}(\tau_2,\tau_1)\begin{pmatrix}B_1 & B_2 \\ B_2 & B_1\end{pmatrix}U_2,$$

where

$$A_{1,2}=\frac{1}{2}\left(\frac{n_1(\mathbf{k})-n_1(\mathbf{k}-\mathbf{q})}{q_0-\mathcal{E}_1(\mathbf{k})+\mathcal{E}_1(\mathbf{k}-\mathbf{q})}\mp\frac{n_2(\mathbf{k})-n_2(\mathbf{k}-\mathbf{q})}{q_0+\mathcal{E}_2(\mathbf{k})-\mathcal{E}_2(\mathbf{k}-\mathbf{q})}\right),$$

$$B_{1,2}=\frac{1}{2}\left(\frac{1-n_2(\mathbf{k})-n_1(\mathbf{k}-\mathbf{q})}{q_0+\mathcal{E}_2(\mathbf{k})+\mathcal{E}_1(\mathbf{k}-\mathbf{q})}\mp\frac{1-n_1(\mathbf{k})-n_2(\mathbf{k}-\mathbf{q})}{q_0-\mathcal{E}_1(\mathbf{k})-\mathcal{E}_2(\mathbf{k}-\mathbf{q})}\right).$$

Write the vertex function as $\Gamma=\sum_{\mu}\gamma_{\mu}\tau_{\mu}$ (and similarly for the bare vertex function), we have

$$\sum_{k_0}G(k)\Gamma_q(k)G(k-q)=(\tau_0,\tau_2,\tau_1,\tau_3)\begin{pmatrix}C^- & S^- & 0 & 0 \\ -S^- & C^- & 0 & 0 \\ 0 & 0 & C^+ & -S^+ \\ 0 & 0 & S^+ & C^+\end{pmatrix}\begin{pmatrix}A_1 & 0 & 0 & A_2 \\ 0 & B_1 & B_2 & 0 \\ 0 & B_2 & B_1 & 0 \\ A_2 & 0 & 0 & A_1\end{pmatrix}$$

$$\times\begin{pmatrix}C^- & -S^- & 0 & 0 \\ S^- & C^- & 0 & 0 \\ 0 & 0 & C^+ & S^+ \\ 0 & 0 & -S^+ & C^+\end{pmatrix}\begin{pmatrix}\gamma_0 \\ \gamma_2 \\ \gamma_1 \\ \gamma_3\end{pmatrix}$$

$$\equiv\hat{\tau}\hat{S}_{\mathbf{q}}^{\dagger}(k)\hat{A}_{\mathbf{q}}(k)\hat{S}_{\mathbf{q}}(k)\hat{\gamma}_{\mathbf{q}}(k).$$

Note that $\hat{S}^{\dagger}$ can be obtained from $\hat{S}$ by reversing the signs of both v_1 and v_2. The equation for the vertex function is then

$$\hat{\gamma}_{\mathbf{q}}(\mathbf{k})=\hat{\gamma}_{\mathbf{q}}^0(\mathbf{k})+\sum_{\mathbf{k}'}\hat{S}_{\mathbf{q}}^{\dagger}(\mathbf{k}')\hat{A}_{\mathbf{q}}(\mathbf{k}')\hat{S}_{\mathbf{q}}(\mathbf{k}')V_S(\mathbf{k}-\mathbf{k}')\hat{\gamma}_{\mathbf{q}}(\mathbf{k}').$$

For a numerical calculation of the ladder diagram at arbitrary wave vector and frequency, it is still quite complex. We shall consider only two special cases.

(1) Let $q_0=0$ and then set $q\rightarrow0$: This allows us to calculate the long-wavelength limit of the screening, since the polarization (density-density correlation) function is related to the vertex function via the same equation as (11) with the bare vertex function replaced by τ_0. We have

$$A_{1,2}=-\frac{1}{2}\left(\frac{dn_1}{d\mathcal{E}_1}\pm\frac{dn_2}{d\mathcal{E}_2}\right),\quad B_1=\frac{1-n_1(k)-n_2(k)}{2E_{\mathbf{k}}},\quad B_2=0.$$

In the case of equal mass, $A_2=0$ and $A_1=-dn(\mathbf{k})/dE_{\mathbf{k}}$. To calculate Π_0, we only need to keep the term proportional to τ_0 and γ_0. If we ignore the ladder diagram contribution, then $\gamma_0=1$, and the polarization can be expressed as

$$\Pi_0=-2\sum_{\mathbf{k}}dn(\mathbf{k})/dE_{\mathbf{k}}.$$

(2) Let $\mathbf{q}=0$ and $q_0\neq0$ (here q_0 is defined as the energy difference between the photon energy and the chemical po-

tential μ): $C^- = 1$, $S^- = 0$, $C \equiv C^+ = u_{\mathbf{k}}^2 - v_{\mathbf{k}}^2 = \epsilon_{\mathbf{k}}/E_{\mathbf{k}}$, and $S \equiv S^+ = 2u_{\mathbf{k}}v_{\mathbf{k}} = \Delta_{\mathbf{k}}/E_{\mathbf{k}}$. This is a case of interest for calculating the optical spectra. Since the photon wave vector $\mathbf{q}$ associated with the transition energies in a semiconductor is typically much smaller compared with the exciton Bohr radius, we can assume that $\mathbf{q} = 0$. We then have $A_1 = A_2 = 0$. Let $\omega_{\mathbf{k}} \equiv 2E_{\mathbf{k}}$ and $N_{\mathbf{k}} \equiv 1 - n_1(\mathbf{k}) - n_2(\mathbf{k})$, we have

$$\sum_{k_0} G(k)\Gamma(k)G(k) \begin{pmatrix} 0 \\ -\omega_{\mathbf{k}}\gamma_2 + q_0(C\gamma_1 + S\gamma_3) \\ C[q_0\gamma_2 - \omega_{\mathbf{k}}(C\gamma_1 + S\gamma_3)] \\ S[q_0\gamma_2 - \omega_{\mathbf{k}}(C\gamma_1 + S\gamma_3)] \end{pmatrix}.$$
(13)

We then have the following equations:

$$\gamma_2(\mathbf{k}) - \sum_{\mathbf{k}'} V_S(\mathbf{k} - \mathbf{k}') \frac{N_{\mathbf{k}'}}{q_0^2 - \omega_{\mathbf{k}'}^2} \{q_0 F_{\mathbf{k}'} - \gamma_2(\mathbf{k}')\omega_{\mathbf{k}'}\}$$
$$= \gamma_2^0(\mathbf{k}),$$

$$\gamma_1(\mathbf{k}) + \sum_{\mathbf{k}'} V_S(\mathbf{k} - \mathbf{k}') \frac{N_{\mathbf{k}'}}{q_0^2 - \omega_{\mathbf{k}'}^2} C_{\mathbf{k}'} \{\omega_{\mathbf{k}'} F_{\mathbf{k}'} - \gamma_2(\mathbf{k}')q_0\}$$
$$= \gamma_1^0(\mathbf{k}),$$

$$\gamma_3(\mathbf{k}) + \sum_{\mathbf{k}'} V_S(\mathbf{k} - \mathbf{k}') \frac{N_{\mathbf{k}'}}{q_0^2 - \omega_{\mathbf{k}'}^2} S_{\mathbf{k}'} \{\omega_{\mathbf{k}'} F_{k'} - \gamma_2(\mathbf{k}')q_0\}$$
$$= \gamma_3^0(\mathbf{k}),$$

where $F_{\mathbf{k}} \equiv C_{\mathbf{k}}\gamma_1(\mathbf{k}) + S_{\mathbf{k}}\gamma_3(\mathbf{k})$. Denote $F_{\mathbf{k}}^0 \equiv C_{\mathbf{k}}\gamma_1^0(\mathbf{k}) + S_{\mathbf{k}}\gamma_3^0(\mathbf{k})$ and $G_{\mathbf{k}} \equiv (\omega_{\mathbf{k}}F_{\mathbf{k}} - q_0\gamma_2)/(q_0^2 - \omega_{\mathbf{k}}^2)$; we have

$$F_{\mathbf{k}} + \sum_{\mathbf{k}'} V_S(\mathbf{k} - \mathbf{k}')(C_{\mathbf{k}}C_{\mathbf{k}'} + S_{\mathbf{k}}S_{\mathbf{k}'})N_{\mathbf{k}'}G_{\mathbf{k}'} = F_{\mathbf{k}}^0, \quad (14)$$

$$\omega_{\mathbf{k}}F_{\mathbf{k}} - (q_0^2 - \omega_{\mathbf{k}}^2)G_{\mathbf{k}} - \sum_{\mathbf{k}'} V_S(\mathbf{k} - \mathbf{k}')N_{\mathbf{k}'}(F_{\mathbf{k}'} + \omega_{\mathbf{k}'}G_{\mathbf{k}'})$$
$$= \gamma_2^0(\mathbf{k})q_0. \quad (15)$$

Substitute Eq. (14) into Eq. (15); we obtain

$$q_0^2 G_{\mathbf{k}} - \sum_{\mathbf{k}'} H_{\mathbf{k},\mathbf{k}'} G_{\mathbf{k}'} = \sum_{\mathbf{k}'} [\omega_{\mathbf{k}}\delta_{\mathbf{k},\mathbf{k}'} - V_S(\mathbf{k} - \mathbf{k}')N_{\mathbf{k}'}]F_{\mathbf{k}'}^0$$
$$- q_0\gamma_2^0(\mathbf{k}),$$

where

$$H_{\mathbf{k}\mathbf{k}'} = \sum_{\mathbf{p}} [\omega_{\mathbf{k}}\delta(\mathbf{k} - \mathbf{p}) - V_S(\mathbf{k} - \mathbf{p})N_{\mathbf{p}}][\omega_{\mathbf{p}}\delta(\mathbf{p} - \mathbf{k}')$$
$$- V_S(\mathbf{p} - \mathbf{k}')(C_{\mathbf{p}}C_{\mathbf{k}'} + S_{\mathbf{p}}S_{\mathbf{k}'})N_{\mathbf{k}'}].$$

$G_{\mathbf{k}}$ can be solved by inverting the matrix $q_0^2 - H_{\mathbf{k}\mathbf{k}'}$. Two facts will be used to simplify the computation. First, only the s-like component of $G_{\mathbf{k}}$ will contribute to the optical spec-

trum, since the system has rotational symmetry. Thus, we can integrate out the angle between $\mathbf{k}$ and $\mathbf{k}'$ and obtain a new H matrix whose indices are the magnitudes of $\mathbf{k}$ and $\mathbf{k}'$. 450 mesh points of k and k' with a cutoff corresponding to $k_C^2 = 100$ Ry will be used to define the H matrix numerically. Second, the inverse of the new matrix $(q_0^2 - H_{kk'})$ can be written as $\sum_{\nu} S_{k\nu}(q_0^2 - w_\nu)^{-1} S_{\nu,k'}^{-1}$, where S is a similarity matrix that diagonalizes H and w_ν denotes the eigenvalues of H.

For the optical absorption process, we have $\Gamma^0(\mathbf{k}) = P(\mathbf{k})\tau^+$; thus, we set $\gamma_1^0 = -\gamma_2^0 = P_{\mathbf{k}}/2$ and $\gamma_0^0 = \gamma_3^0 = 0$. The absorption coefficient is given by the imaginary part of the coefficient of $\tau^+ = (\tau_1 - \tau_2)/2$ in Eq. (13) multiplied by $P(\mathbf{k})$, viz.,

$$\alpha(q_0) \propto -\text{Im} \sum_{\mathbf{k}} P^*(\mathbf{k})N_{\mathbf{k}}\left[C_{\mathbf{k}}G_{\mathbf{k}} + \frac{1}{q_0}(F_{\mathbf{k}} + \omega_{\mathbf{k}}G_{\mathbf{k}})\right].$$

For comparison, we shall also calculate the optical spectra without the exciton effects. In this case, γ_μ will be replaced by γ_μ^0 in Eq. (13) and the absorption coefficient reduces to

$$\alpha(q_0) \propto -\text{Im} \sum_{\mathbf{k}} |P(\mathbf{k})|^2 \frac{N_{\mathbf{k}}}{q_0^2 - \omega_{\mathbf{k}}^2}\left\{\frac{q_0\epsilon_{\mathbf{k}}}{E_{\mathbf{k}}} + 2E_{\mathbf{k}}\left[1 + \left(\frac{\epsilon_{\mathbf{k}}}{E_{\mathbf{k}}}\right)^2\right]\right\}.$$

In the zero-temperature limit, this reduces to the expression considered in Ref. 9 except that here $\epsilon_{\mathbf{k}}$ also includes the Hartree-Fock exchange energy. In realistic systems, all excitations have a finite lifetime, which can be simulated by letting $q_0 \to q_0 + i\Lambda$, where Λ is the half-width of the broadening. Throughout the paper, the broadening parameter used is $\Lambda = 0.5$ Ry. Note at $q_0 = 0$ (when the photon energy equals μ), the function $G_{\mathbf{k}}$ contains a singularity of the type $1/q_0^2$ due to the Goldstone mode (the condensate state). The imaginary part of this gives rise to a function $2q_0\Lambda/(q_0^2 + \Lambda^2)$ when we make the substitution $q_0 \to q_0 + i\Lambda$. This result is unphysical, since the term represents equal emission and absorption at the same energy and it should give zero contribution. To remedy this, we simply locate the Goldstone mode and remove its $1/q_0^2$ contribution in our numerical calculation.

Figure 3 shows the calculated zero-temperature absorption spectra of the exciton condensate in the 3D system with input chemical potentials $\mu = -1$, -0.5, 0, 0.5, and 1 Ry. The corresponding densities for these curves are $N_0 = 0, 0.022, 0.049, 0.079, 0.112a_B^{-3}$ For comparison results both with and without the exciton effect are shown. In the plot, a negative absorption coefficient indicates gain. At the zero-density limit, only the spectrum with the exciton effect is shown and it is the same as the absorption spectrum of a hydrogenic exciton in 3D, which has an exciton peak at $E = -1$ Ry and goes as $\sqrt{E}$ at the high-energy limit. As expected the exciton effect is quite significant in both the absorption and gain. When the exciton effect is included, a sharp exciton peak is seen in the absorption spectra followed by a secondary peak, which is caused by the singularity in the joint density of states $D(E)$ of the quasiparticles due to the formation of a gap. Note that if we ignore the wave-vector dependence of the gap $\Delta_{\mathbf{k}}$, then
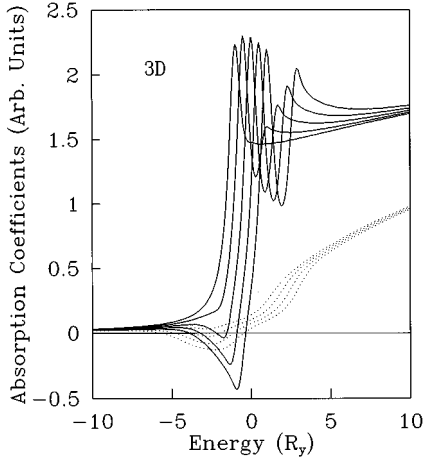
FIG. 3. Absorption spectra of the exciton condensate in 3D with input chemical potentials $\mu = -1, -0.5, 0, 0.5$, and 1 Ry. Solid curves: with the exciton effect. Dotted curves: without the exciton effect. The curves with exciton peaks located at higher energies correspond to higher μ. The corresponding densities for these curves are $N_0 = 0, 0.022, 0.049, 0.079, 0.112 a_B^{-3}$.

$$D(E) = \sum_{\mathbf{k}} \delta(E - 2E_{\mathbf{k}}) = \sum_{\mathbf{k}} \delta(\epsilon - 2\epsilon_{\mathbf{k}}) / |dE_{\mathbf{k}}/d\epsilon_{\mathbf{k}}|$$

$$\propto E / \sqrt{E - 2\Delta}$$

as $E \to 2\Delta$. This singularity is further enhanced by the exciton effect. We have also confirmed numerically that the energy separation between the secondary peak and the exciton peak is very close to the average value of the gap $2\Delta_{\mathbf{k}}$. Without the exciton effect, the singularity is quite weak and the peak structure has been smeared out by the broadening. The gain always occurs below the exciton peak, which is due to the recombination of an exciton in the condensate while shaking an exciton into one of the excited noncondensate states. The position of maximum gain is also roughly 2Δ below the exciton peak.

Figure 4 shows the calculated zero-temperature absorption spectra of the exciton condensate in the ideal 2D system with input chemical potentials $\mu = -4, -3.5, -3, -2.5$, and -2 Ry. The corresponding densities for these curves are $N_0 = 0, 0.084, 0.164, 0.240, 0.314 a_B^{-2}$. At the zero-density limit, the absorption spectrum of a hydrogenic exciton in 2D (which has an exciton peak at $E = -4$ Ry and a steplike spectrum at the high-energy limit) is reproduced. The absorption coefficient is normalized so that the step height is 1 at the high-energy limit. The exciton effect is found to be even more significant in the 2D case as demonstrated by the stronger exciton peaks. The secondary peak (for finite densities) is again caused by the singularity in the joint density of states $D(E)$ of the quasiparticles. In this case

$$D(E) \propto E / \sqrt{E^2 - 4\Delta^2},$$

which shows a stronger singularity than the 3D case. Although this singularity is further enhanced by the exciton effect, it is still prominent even without the exciton effect. A major difference between the results with and without the exciton effect is the prediction of the position of maximum
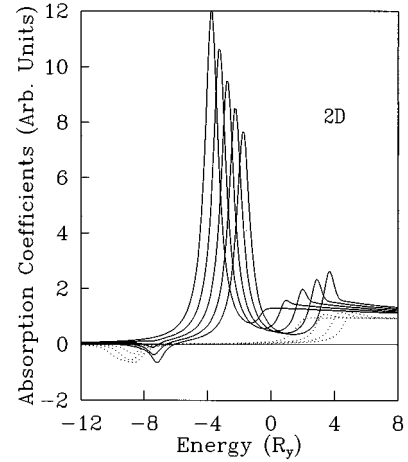
gain. Without the exciton effect, the gain peaks at around -9 Ry, whereas with the exciton effect, the position shifts to around -7 Ry for the densities considered here. It is expected that when the full screening effect is included, the result should be somewhere between the two. In either case, lasing below the free exciton line is predicted, consistent with the experimental observations.[8]

The quasi-2D system can be realized in semiconductor quantum wells. The interaction for a quasi-2D system can be well approximated by the form $V(\mathbf{q}) = a/q(1+qb)$ with b being a parameter comparable to the size of the quantum well.[12] Note that the additional factor $(1+bq)$ behaves like a short-range screening of the 2D Coulomb potential. Figures 5 and 6 show the calculated zero-temperature absorption spectra of the exciton condensate in two different quasi-2D

FIG. 4. Absorption spectra of the exciton condensate in 2D with input chemical potentials $\mu = -4, -3.5, -3, -2.5$, and -2 Ry. $T = 0$ K. Solid curves: with the exciton effect. Dotted curves: without the exciton effect. The curves with exciton peaks located at higher energies correspond to higher μ. The corresponding densities for these curves are $N_0 = 0, 0.084, 0.164, 0.240, 0.314 a_B^{-2}$.
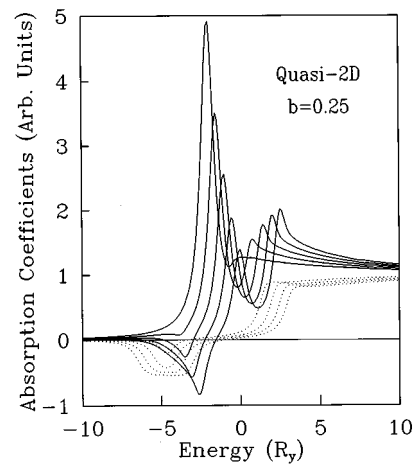

FIG. 5. Absorption spectra of the exciton condensate in quasi-2D with input chemical potentials $\mu = (-2.03 + 0.5n)$ Ry; $n = 0, 1, 2, 3, 4$ and interaction parameter $b = 0.25 a_B$. $T = 0$ K. Solid curves: with the exciton effect. Dotted curves: without the exciton effect. The corresponding densities for these curves are approximately $N_0 = 0, 0.083, 0.156, 0.223, 0.286 a_B^{-2}$.
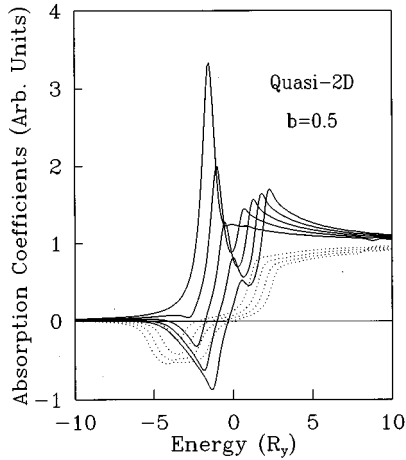
FIG. 6. Absorption spectra of the exciton condensate in quasi-2D with input chemical potentials $\mu=(-1.54+0.5n)$ Ry; $n=0,1,2,3,4$ and interaction parameter $b=0.5a_B$. $T=0$ K. Solid curves: with the exciton effect. Dotted curves: without the exciton effect. The corresponding densities are approximately $N_0=0,0.082,0.149,0.210,0.267a_B^{-2}$.

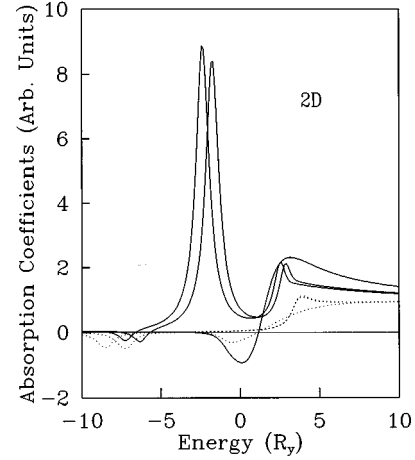
FIG. 7. Absorption spectra of the exciton condensate in 2D with approximately the same density $(0.2\ a_B^{-2})$, but different temperatures $(T=0.375, 0.525, 0.675$ Ry$/k_B)$. Solid curves: with the exciton effect. Dotted curves: without the exciton effect. The curves with maximum gain located at higher energies correspond to higher T.

systems with input chemical potentials $\mu=-E_B+0.5\ n$ Ry; $n=0,1,2,3,4$, where E_B is the exciton binding energy in the zero-density limit. E_B are 2.03 and 1.54 Ry for these two cases. Note that exciton binding energies in typical quantum wells are in the range of $1.5-2.5$ Ry. The corresponding densities for these curves are $N_0=0$, $0.083,0.156,0.223,0.286\ a_B^{-2}$ for $b=0.25a_B$ in Fig. 5 and $N_0=0,0.082,0.149,0.210,0.267a_B^{-2}$ for $b=0.5a_B$ in Fig. 6. As expected, the main features are similar to the ideal 2D case, with weaker exciton effect as the value of the b parameter increases. Without the exciton effect, the gain spectra are quite broad. With the exciton effect the gain spectra become narrower and the position of maximum gain shifts to higher energy. This is due to the fact that the density of states for the excited exciton states tends to pile up near the minimum excitation energy, which is less than 2Δ when the exciton effect is included. At low densities $(0.1a_B^{-2}<N_0<0.2a_B^{-2}$ or 5×10^{11} cm$^{-2}<N_0<10^{12}$ cm^{-2} for ZnSe systems) lasing below the free exciton (FE) line is predicted. Just above the critical density (below which the gain is zero), the position of maximum gain is estimated (according to our theory) to be around $1-2$ Ry (or $17-34$ meV for ZnSe) below the FE line for most semiconductor quantum-well systems. This position shifts up toward the FE line as the density increases from the critical density.

Experimentally,[8] it was found that for ZnSe quantum-well systems, lasing does occur at about 15 meV below the free-exciton absorption line for a density around 7×10^{11} cm^{-2}. This is consistent with the results obtained here. However, to make a quantitative comparison between theory and experiment, one must also consider the following factors: (1) the laser emission spectrum may arise from excitons localized by interface roughness as proposed in Ref. 2,8, the short-range screening ignored in the calculation may cause the exciton gain peak to shift toward lower energy so the result is closer to that without the exciton effect, and and (3) the biexciton states, which are ignored in the present calculation, may also contribute to a below-exciton peak in the gain spec-

trum (this can happen when one exciton recombines while breaking up the other exciton during the process).

Figure 7 shows the calculated absorption spectra with and without exciton effect for a fixed density at three different temperatures (with equal separations), two below T_c and one above T_c. The static screening due to the unpaired electrons and holes is included. The overall shape is not much different in the two cases with $T<T_c$, whereas a significant change is noticed when $T>T_c$, reflecting the phase transition. As long as $T<T_c$, the position at maximum gain shifts up by about 1 Ry when the exciton effect is included. The position of the exciton peak in the absorption (gain) spectrum shifts upward with increasing temperature, since it is tied to the chemical potential in our theory, which increases with T (below what would be the value if a free Fermi gas theory was used, however, see Fig. 1). In contrast, for $T>T_c$ the chemical potential decreases with increasing temperature similar to the Fermi gas system. For $T>T_c$, the condensation effects have vanished, but the exciton effect remains present.

IV. FLUCTUATION EFFECTS ON BOSE CONDENSATION

It is well known that boson condensation is not favorable in low dimensions. One remaining question is whether there is still boson condensation at finite temperature for excitons in 2D structures. We will present in the following the analysis that shows that boson condensation is indeed possible for electron-hole systems only. The same analysis shows that condensation of Cooper pairs is not possible. The main difference is the form of the interaction, which has already been pointed out earlier. In the Cooper pairing case, fluctuations come from the vertex correction while in the exciton condensations, fluctuations come from the dressed interaction.

It has been shown that[13] the current conservation leads to the following Ward-Takahashi identity:

$$q_\mu\Gamma_q^\mu(k)=\tau G^{-1}(k)-G^{-1}(k-q)\tau,$$

where $\tau=\tau_0$ for the exciton case and $\tau=\tau_3$ for the super-conductivity case. Γ^μ are the three-point vertex functions related to the charge density ρ and current $\mathbf{J}$ with $\rho(x)\equiv\bar{\psi}(x)\tau\psi(x)$. For the exciton system at zero momentum transfer $\mathbf{q}=0$ and $q_0\to0$, we have $\Gamma^0_{q_0=0}(k)=\partial G^{-1}(k)/\partial k_0=\tau_0$, which is finite. Therefore vertex correction is not important as far as the gap equation is concerned. However, since $\tau=\tau_3$ for Cooper pairs, the off-diagonal elements of $\Gamma^0_{q_0}(k)$ are proportional to $2\Delta_\mathbf{k}/q_0$, which diverges as $q_0\to0$; therefore, the vertex correction is very important. Including the vertex correction in the gap equation would not allow a nonzero solution for $\Delta_\mathbf{k}$. Thus, Bose condensation cannot exist in 2D for the Cooper pairs. For the exciton system, we shall ignore the vertex function and consider other fluctuation effects.

A careful analysis also shows that the dressed interaction would not cause any divergence in the Cooper pair condensations. Compared to the vertex correction, the fluctuation effect of fully dynamically dressed interaction is more important for the exciton system. In the following we will analyze the dressed interaction for the excitons and show that it will not destroy the Bose condensation. Assume that the density-density correlation is rewritten in the general form

$$\Pi(q)=q^2\int d\omega\frac{\rho_\mathbf{q}(\omega)}{(q_0+i0)^2-\omega^2},$$

where the factor q^2 is put in according to the sum rule for the imaginary part of the density-density correlation function so that

$$\int d\omega\omega\text{Im}\Pi(\mathbf{q},\omega)\propto N_0q^2,$$

where N_0 is the total pair density and independent of the wave vector q.

With the vertex correction ignored, the self-energy correction beyond Hartree-Fock theory is given by

$$\Sigma^{(c)}(k)=\sum_q V^2(\mathbf{q})\Pi(q)\tau G(k-q)\tau$$

$$=\int d\omega\sum_\mathbf{q} V^2(\mathbf{q})q^2\frac{\bar{\rho}_\mathbf{q}(\omega)}{2\omega}\frac{1-n(\mathbf{k}-\mathbf{q})+N(\omega)}{k_0^2-(E_{\mathbf{k}-\mathbf{q}}+\omega)^2}$$

$$\times\left[k_0+\frac{E_{\mathbf{k}-\mathbf{q}}+\omega}{E_{\mathbf{k}-\mathbf{q}}}(\epsilon_{\mathbf{k}-\mathbf{q}}\tau_3+\sigma\Delta_{\mathbf{k}-\mathbf{q}}\tau_1)\right],$$

where $\bar{\rho}_\mathbf{q}(\omega)=\rho_\mathbf{q}(\omega)+\rho_\mathbf{q}(-\omega)$ and $N(\omega)=1/(e^{\beta\omega}-1)$. Here we are only concerned with the exciton system, we choose $\tau=\tau_0$ and $\sigma=1$. If the Cooper pair condensation is of interest, we shall simply set $\tau=\tau_3$ and $\sigma=-1$ in the above equation. The self-energy is meaningful only when the frequency is replaced by the on-shell energy. Including the $\Sigma^{(c)}(E_\mathbf{k})$ contribution to the self-consistent equations (6) and (8), we obtain

$$\epsilon_\mathbf{k}=\epsilon_\mathbf{k}^0-\frac{1}{2}\sum_\mathbf{q} V(\mathbf{k}-\mathbf{q})\left[1-[1-2n(\mathbf{q})]\frac{\epsilon_\mathbf{q}}{E_\mathbf{q}}\right]$$

$$+\int d\omega dq V^2(\mathbf{q})q^2\frac{\bar{\rho}_\mathbf{q}(\omega)}{2\omega}\frac{1-n_{\mathbf{k}-\mathbf{q}}+N(\omega)}{E_\mathbf{k}^2-(E_{\mathbf{k}-\mathbf{q}}+\omega)^2}$$

$$\times\left(\epsilon_\mathbf{k}+\frac{E_{\mathbf{k}-\mathbf{q}}+\omega}{E_{\mathbf{k}-\mathbf{q}}}\epsilon_{\mathbf{k}-\mathbf{q}}\right),$$

$$\Delta_\mathbf{k}=\sigma\frac{1}{2}\sum_\mathbf{q} V(\mathbf{k}-\mathbf{q})[1-2n(\mathbf{q})]\frac{\Delta_\mathbf{q}}{E_\mathbf{q}}$$

$$+\int d\omega\sum_\mathbf{q} V^2(\mathbf{q})q^2\frac{\bar{\rho}_\mathbf{q}(\omega)}{2\omega}\frac{1-n(\mathbf{q})+N(\omega)}{E_\mathbf{k}^2-(E_{\mathbf{k}-\mathbf{q}}+\omega)^2}$$

$$\times\left(\Delta_\mathbf{k}+\sigma\Delta_{\mathbf{k}-\mathbf{q}}\frac{E_{\mathbf{k}-\mathbf{q}}+\omega}{E_{\mathbf{k}-\mathbf{q}}}\right).$$

A careful analysis shows that there is no divergence in the gap equation whether $V(0)=$ const or $V(q)\propto1/q$ at small q. For small $\mathbf{q}$ and ω, $\rho_\mathbf{q}(\omega)$ is sharply peaked at the plasma frequency $\omega_\mathbf{q}$. For the ideal 2D system $V(q)\propto1/q$ and plasma frequency goes like $\omega_\mathbf{q}\propto q^{1/2}$. The integral over ω in the above equation leads to a divergent term of the order $1/\omega_\mathbf{q}^3\propto q^{3/2}$. [Note that $N(\omega)\to1/\omega$ as $\omega\to0$]. Finally, carrying out the momentum integration leads to a finite result, which goes like $\int dq/q^{1/2}\approx2q^{1/2}$.

V. SUMMARY

In summary we have solved the Bose condensation of excitons at finite temperatures including the static screening effects and calculated the optical absorption (gain) spectra including the exciton effect (vertex correction). For ideal 2D systems, the Bose condensation can exist up to $T=30$ K (130 K) for GaAs (ZnSe) parameters. For typical quantum wells (quasi-2D systems), the transition temperatures are expected to be somewhat lower. The optical spectra for 3D, 2D, and quasi-2D systems at zero temperature are studied, and the exciton effect gives rise to significant modification to both the absorption and gain spectra. For quasi-2D systems lasing below the free exciton line is predicted and the position of maximum gain is consistent with experimental observation. The temperature dependence of the optical spectra for the ideal 2D system is examined, and the spectrum shows a marked change when the temperature moves across T_c, indicating the significant effect of the Bose condensation on optical spectra. These effects should be experimentally observable. By including the fluctuation effects, we have also shown that Bose condensation of excitons is possible for two-dimensional systems contrary to the case of Cooper-pair condensation.

[1] J.L. Lin and J.P. Wolfe, Phys. Rev. Lett. **71**, 1222 (1993).

[2] M.H. Anderson, J.R. Ensher, M.R. Mathews, C.E. Wieman, and E.A. Cornell, Science **269**, 198(1995).

[3] R.J. Schrieffer, *Theory of Superconductivity* (Benjamin, New York, 1964).

[4] L.V. Keldysh and A.N. Kozlov, Zh. Éksp. Teor. Fiz. **54**, 978 (1968) [Sov. Phys. JETP **27**, 521(1968)].

[5] R. Zimmermann, Phys. Status Solidi B **76**, 191 (1976).

[6] C. Comte and P. Noziéres, J. Phys (Paris) **43**, 1069(1982).

[7] X. Zhu, P.B. Littlewood, M.S. Hybertsen, and T.M. Rice, Phys. Rev. Lett. **74**, 1633 (1995).

[8] J. Ding, M. Hagerott, T. Ishihara, H. Jeon, and A. V. Nurmikko, Phys. Rev. B **47**, 10 528 (1993), and references therein.

[9] M.E. Flatté, E. Runge, and H. Ehrenreich, Appl. Phys. Lett. **66**, 1313(1995).

[10] G. Baym and L. P. Kadanoff, Phys. Rev. **124**, 287 (1961).

[11] See, for example, G. D. Mahan, *Many-Particle Physics* (Plenum, New York, 1981).

[12] G. D. Sanders and Y. C. Chang, Phys. Rev. B **35**, 1300 (1987).

[13] H. Chu, H. Umezawa, and F.C. Khanna, Phys. Lett. A **191**, 174 (1994).